Metabolomics (2019) 15:26
https://doi.org/10.1007/s11306-019-1491-8

ORIGINAL ARTICLE

Global urinary metabolic profiling of the osteonecrosis of the femoral head based on UPLC–QTOF/MS

Gang Yang[1] · Gang Zhao[1] · Jian Zhang[2] · Sichuan Gao[2] · Tingmei Chen[3] · Shijia Ding[3] · Yun Zhu[1]

Received: 22 September 2018 / Accepted: 13 February 2019 / Published online: 20 February 2019

Abstract

Introduction Osteonecrosis of the femoral head (ONFH), one of the widespread orthopedic diseases with a decrease in bloodstream to the femoral head, is frequently accompanied by cellular death, trabecula fracture, and collapse of the articular surface. The exactly pathological mechanism of ONFH remains to explore and further identify.

Objectives The aim was to identify the global urinary metabolic profiling of ONFH and to detect biomarkers of ONFH.

Methods Urine samples were collected from 26 ONFH patients and 26 healthy people. Ultra-performance liquid chromatography–quadrupole time of flight tandem mass spectrometry (UPLC-QTOF/MS) in combination with multivariate statistical analysis was developed and performed to identify the global urinary metabolic profiling of ONFH.

Results The urinary metabolic profiling of ONFH group was significantly separated from the control group by multivariate statistical analysis. 33 distinctly differential metabolites were detected between the ONFH patients and healthy people. Sulfate, urea, Deoxycholic acid and PE(14:0/14:1(9Z)) were screened as the potential biomarkers of ONFH. In addition, the up/down-regulation of sulfur metabolism, cysteine and methionine metabolism, glycerophospholipid metabolism, and histidine metabolism were clearly be associated with the ONFH pathogenic progress.

Conclusion Our results suggested that metabolomics could serve as a promising approach for identifying the diagnostic biomarkers and elucidating the pathological mechanism of ONFH.

Keywords Metabolomics · UPLC–MS/MS · Osteonecrosis of the femoral head · Urine · Biomarkers

1 Introduction

Osteonecrosis of the femoral head (ONFH), also known as avascular necrosis, is a widespread orthopedic disease with a decrease in bloodstream to the femoral head, frequently accompanied by cellular death, trabecula fracture, and collapse of the articular surface (Calder et al. 2004; Levasseur 2008; Powell et al. 2011). Two categories of ONFH are reported, traumatic and nontraumatic (Moya-Angeler et al. 2015). It mostly affects relatively young people, resulting irreversible dysfunction of the hip joint and impairing quality of life (Mankin 1992; Slobogean et al. 2015). Thus, the total hip arthroplasty (THA) is the only definitive treatment for this disease (Zalavras et al. 2014). Epidemiological study shows that 500–700 million people were suffering from nontraumatic ONFH in China and approximately 100,000–200,000 new cases were diagnosed annually (Cui et al. 2016; Liu et al. 2017). Predisposing risk factors, such as alcohol consumption, trauma, corticosteroid use, autoimmune diseases, coagulation disorders, smoking, hemoglobinopathies, dysbaric phenomena, hyperlipidemia, storage diseases, have been confirmed (Hernigou et al. 2015; Shah et al. 2015; Wen et al. 2017). However, the pathogenesis and etiology of osteonecrosis are not completely understand. Ischemia, direct cellular toxicity, and altered differentiation of mesenchymal stem cells are recognized three

Electronic supplementary material The online version of this article (https://doi.org/10.1007/s11306-019-1491-8) contains supplementary material, which is available to authorized users.

✉ Yun Zhu
zhuyun79@163.com

[1] Department of Orthopedics, Fuling Center Hospital of Chongqing City, Chongqing 408000, China

[2] Department of Orthopedics, The First Affiliated Hospital, Chongqing Medical University, Youyi Road No. 1, Chongqing 400016, China

[3] Key Laboratory of Clinical Laboratory Diagnostics (Ministry of Education), College of Laboratory Medicine, Chongqing Medical University, Chongqing 400016, China

major pathogenic mechanisms (Zalavras et al. 2000; Glueck et al. 2008; Lee et al. 2006). Bone marrow cell necrosis, marrow structure disturbance, fibrosis invasion, and empty lacunae appearance in trabecula are the typical histopathological changes of ONFH (Kang et al. 2015; Qiang et al. 2015; Ragab et al. 2008). X-ray, Computed tomography (CT) scanning and Magnetic Resonance Imaging (MRI) are recommended as the routine diagnostic approaches (Stevens et al. 2003). The invasively histopathological examination is the diagnostical golden standard (Sugano et al. 1999). Early diagnosis for ONFH patient still remains a worldwide problem, especially the patient with predisposing risk factors. Thus, a new non-invasive approach to explore this disease is urgently needed to understand ONFH thoroughly.

Systems biology supported by genomics, proteomics, metabolomics, and bioinformatics, provides a new logical framework to illuminate disease etiology and to discover the potential connection between seemingly disparate disease states (De Preter 2015; Holmes et al. 2008; Wilson 2014; Loscalzo et al. 2007). Metabolomics, one branch of the systems biology, has been widely performed in biomedical research for more than a decade (Patti et al. 2012; Snyder et al. 2013). It allows the quantification of hundreds of organic and inorganic metabolites, small molecules downstream of biochemical pathways (Issaq et al. 2009). To allow rapid and extensive analysis of small molecule metabolites with biological sample preparation, Mass Spectrometry combined with chromatographic separation and Nuclear Magnetic Resonance are the frequently used analytical platforms for metabolic analysis (Schuhmacher et al. 2013). As a novel strategy for discovery of biomarkers of interest, metabolomics has been successfully used in diagnostics, physiology, functional genomics, pharmacology, nutrition, and toxicology (Puchades et al. 2015; Zhang et al. 2012; Winder et al. 2011), because of its sensitivity and quantitative reproducibility. Compared to the conventional liquid chromatography, the ultra-performance liquid chromatography (UPLC) obtains an even rapid separation, higher resolution, and higher sensitivity (Grauso et al. 2015).

Metabolic perturbations in plasma and bone tissue from ONFH patients had been discovered based on metabolic analytical technologies (Liu et al. 2016; Xu et al. 2017; Zhu et al. 2016). Plasma samples from patients with ONFH were studied using a combination of high-throughput gas- and liquid-chromatography equipped with mass spectrometry analysis. 123 significantly differential metabolites were detected in ONFH patients compared with the control subjects (Liu et al. 2016). Bone trabecula tissue samples from patients with ONFH were analyzed based on UPLC–MS/MS. 67 differential metabolites were identified between ONFH patients and normal subjects. L-proline, D-arginine, inosine, and L-carnitine, were recommended for diagnostic biomarkers of ONFH (Zhu et al. 2016). In addition, serum metabolomic study was performed in non-traumatic osteonecrosis of the femoral head (NTONFH) based on UPLC–QTOF–MS. 33 significantly differential metabolites were detected in NTONFH group. The combination of LysoPC (18:3), L-tyrosine and L-leucine was proved to have a high diagnostic value for early-stage NTONFH (Xu et al. 2017). In current studies, some evidence of metabolic alterations had shown to be highly associated with ONFH. However, no systematic and comprehensive analysis has been performed to identify the urinary metabolomic characteristics in ONFH patients.

In this study, urine samples from 26 ONFH patients and 26 healthy people were collected. Metabolic profiling analysis based on ultra-performance liquid chromatography coupled with quadrupole-time of flight tandem mass spectrometry was performed. The potential metabolites which were contributed to the discrimination between ONFH patients and healthy people were identified by multivariate statistical analysis. The metabolic profiling was performed to determine the complex dysregulation of the metabolism in ONFH patients, with the purpose to explore the underlying pathogenesis and biomarkers of this disease.

2 Materials and methods

2.1 Experimental participants

The study participants are composed of 26 ONFH patients and 26 healthy people as controls. The ONFH patients were recruited from the inpatients of Department of Orthopedics of The First Affiliated Hospital of Chongqing Medical University from February 2017 to February 2018. The eligibility criteria of participants were as follows: (1) ONFH was diagnosed by the X-ray, CT and MRI with a stage III or IV on the Ficat classification system, (2) the internal and external rotation functions of hip joint were seriously restricted, needed a THA. The exclusion criteria of participants were as follows: (1) Patients had history or evidence of metabolic bone diseases, including serious osteoporosis, Paget's disease, hyper- or hypo-parathyroidism, renal osteodystrophy, bone tumors, presence of cancers with bone metastasis, and so on, (2) patients who reject to participate in this study project. Finally, 26 subjects (9 females/17 males) were included in the ONFH group. For the control group, 26 healthy subjects (10 females/16 males) were enrolled from the outpatients who normally came for the physical examination.

The X-ray, CT, and MRI were commonly used in the diagnosis of ONFH patients. Furthermore, the 26 surgical bone specimens must be immediately collected after the ONFH patients undergo the THA surgery. And then the surgical bone specimens were processed according to the standard histopathological protocols and performed the

histopathological examination. Histopathological reviews of the corresponding surgical bone specimens were performed for all the ONFH patients enrolled in this study. Histopathological examination was used as the gold standard for diagnostics.

2.2 Urine sample preparation

Second morning voided urine specimens were obtained from ONFH patients and control subjects before breakfast. Sodium azide (0.05% wt/vol) was immediately added in urine sample to prevent or inhibit the microbial degradation of the sample. The urine specimens were transferred on dry ice. And then urine specimens were stored in the refrigerator (− 80 °C) to avoid metabolite decay until metabolic analysis. With the purpose to minimize potential alteration of metabolite compositions in urine sample before the solvent extraction, all urine samples were thawed on ice at room temperature for 25 min. 100 µL urine was used for sample preparation according to the suggested protocol (Want et al. 2010). 100 µL acetonitrile was added to precipitate the proteins or other high molecular mass compounds. Ten minutes centrifugation at a speed of 12,000 r/min was applied to remove particulates (4 °C). And then 40 µL supernatant was taken to dilute with 60 µL distilled water. 60 µL of resulting supernatant was transferred into the glass auto-sampler vial. The QC vial was consist of 10 µL of resulting supernatant of each sample.

2.3 UPLC–QTOF/MS analysis

UPLC–QTOF/MS analysis were performed based on a Shimadzu UPLC-equipped AB-Sciex Triple TOF 4600 in both negative and positive ionization modes using the Turbo V ESI ion source. The Triple TOF samples were injected into a Kinetex XB-C18 column (2.1 × 100 mm, 2.6 µm, Phenomenex) and a Kinetex HILIC column (2.1 mm × 100 mm, 2.6 µm, Phenomenex) at a flow rate of 350 µL/min. For the Reversed-phase chromatography, the mobile phase consisted of solvent A (0.1% formic acid in water, v/v) and solvent B (0.1% formic acid in acetonitrile, v/v). The elution conditions were as follows: 0.0–1.0 min, 1% solvent B; 1.0–8.0 min, 5–85% solvent B; 8.0–12.0 min, 85% solvent B; 12.0–12.1 min, 85–5% solvent B; and all the method stopped at 15 min. For the HILIC chromatography, the mobile phase consisted of solvent C [95:5 water–acetonitrile (v/v) with 0.1% formic acid] and solvent D [5:95 water–acetonitrile (v/v) with 0.1% formic acid]. The elution conditions were as follows: 0.0–1.0 min, 95% solvent D; 1.0–8.0 min, 95–50% solvent D; 8.0–12.0 min, 50% solvent D; 12.0–12.1 min, 50–95% solvent D; and all the method stopped at 15 min. The turbo gas (air) and nebulizer gas (air) were set to 55 psi, respectively. The heater temperature was set to 600 °C. The ion spray voltage was set to 5500 V for positive ion and − 4500 V for negative ion mode, respectively. The curtain gas (nitrogen) was set at 25 psi, and the rolling collision energy (CE) was set at 40 ± 15 V for positive ion mode and − (40 ± 15) V for negative ion mode. Full scan analysis was conducted in the electrospray ionization mass spectrometry mode using electrospray ionization technique with coverage of mass range 50–1000 Da, with a scan time equal to 0.25 s for MS scan and 0.1 s for MS/MS scan. 8 data were acquired in one acquisition. The injection volume was 5 µL. The autosampler was maintained at 4 °C during the analysis. The quality control sample (QC), the mixture of equal amounts (10 µL) of each sample, was used for assessing the repeatability and stability of the UPLC–QTOF/MS analytical platform.

2.4 Assessment of analytical method

The QC sample was used for assessing the repeatability and stability of the UPLC–QTOF/MS analytical platform. Ten QC samples were performed to ensure that the analytical system had reached equilibrium before the sample batch. And then, one QC sample was performed at regular five samples intervals to monitor the UPLC–QTOF/MS analytical system. The blank sample (consist of distilled water) was then performed following the interval QC sample, with the purpose to monitor the lack of cross-contamination and for background correction. Principal component analysis (PCA) were performed in QC data sets to evaluate the repeatability and stability of the analytical system. In addition, relative standard deviation (RSD%) of randomly picked peaks from the within-run QC samples in RPLC_Neg, HILIC_Neg, RPLC_Pos, and HILIC_Pos ion modes was performed to assess the reproducibility of the ions, respectively.

2.5 Data preprocessing and analysis

The ion features of metabolites were extracted, pretreated (denoising, baseline correction, alignment, deconvolution) and normalized using the MarkerView v1.2.1 software (AB SCIEXTM, USA). The ''80% rule'' was used for removing the missing peaks (Bijlsma et al. 2006). Principal component analysis (PCA) and Orthogonal Partial Least-squares discrimination analysis (OPLS-DA) were performed for the multivariate statistical analysis using the SIMCA-P 13.0 version software (Umetrics AB, Umeå, Sweden). The variable importance in projection (VIP) value of OPLS-DA models and p value of Mann–Whitney U test were used for separating the two groups. The feature ions with VIP > 1 showed a higher force than average on the classification. Those metabolites (VIP > 1) were eventually picked out as the potential metabolites. Identification the potential metabolites was based on accurate mass, retention time, MS and

MS/MS information. The PeakView software was used for facilitating the MS and MS/MS spectra analysis process by way of chemically intelligent peak-matching algorithms. The potential metabolites were identified based on the following approaches: (a) comparison with fragmentation reported in literature, (b) spectral matching with the Metlin library (http://www.metlin.scripps.edu/) or Mass Bank database (http://www.massbank.jp/), (c) comparison with the MS and MS/MS spectra structure message of the metabolites obtained from the HMDB database (http://www.hmdb.ca/) based on PeakView software, (d) retention time and MS/MS spectra matching with standard reference materials. The clinical diagnostic performance of all changed metabolites were analyzed by performing the receiver operating characteristic (ROC) curve. The statistical analysis of both clinical data and metabolomics data was performed by the SPSS19.0 software. Ultimately, the metabolic pathway analysis was conducted using MetaboAnalyst 4.0 (http://www.metpa.metabolomics.ca./MetPA/faces/Home) based on database source including the HMDB, METLIN, KEGG (http://www.genome.jp/kegg/), and SMPD (http://www.smpdb.ca/) for confirming the related metabolic pathways and visualization.

3 Results

3.1 Clinical characteristics and demographics

The clinical characteristics and demographics of ONFH group and control group were displayed in Table S1. No significant difference was found in age, gender and Body Mass Index (BMI) between ONFH subjects and control subjects. In ONFH subjects, 12 patients had a history of alcohol consumption. 6 patients had a history of fracture of intertrochanteric femoral or femoral neck. 5 patients had a history of corticosteroid treatment. For the rest three ONFH patients, no specific causes were confirmed. ONFH subjects were all staged in III or IV according to the Ficat classification system and the function of activity was seriously restricted. The surgery of THA was conducted in all ONFH patients.

3.2 Medicine images and histopathological analysis

The results of X-ray, CT and MRI images were typically matched with the ONFH histopathological reviews. The X-ray, CT, and MRI images of hip joint were used for clinical diagnosis. And the microscopic images (4×) of eosin-stained and hematoxylin sections of ONFH bone specimen were used for histopathological diagnosis. All the images were presented in Fig. 1. In Fig. 1a, collapse of the femur head was showed in the plain radiograph obtained from the ONFH patients. In Fig. 1b, the trabecula fracture of ONFH femoral head was presented in CT. In Fig. 1c, the typically subchondral fracture as a band of low signal intensity was displayed in T1-weighted MRI image. In Fig. 1d, pathological section showed the lesion region of ONFH femoral head.

3.3 Analytical method repeatability and stability

Sixty-four quality control samples were performed to assessing the repeatability and stability of the UPLC–QTOF/MS analytical platform. R2Ycum of 0.621 and Q2Ycum of 0.576 was obtained in the unsupervised principle component analysis (PCA) model. In PCA model, the QC samples were closely clustered in four separately small spaces in accordance with the four detection ion modes (Fig. S1). The result indicated that the reproducibility of the analytical system was acceptable. In addition, relative standard deviation (RSD%) of eight randomly picked peaks in the six within-run QC samples was used for the evaluation of ions reproducibility. In RPLC-Neg, RPLC-Pos, HILIC-Neg, HILIC-Pos ion modes, the fluctuation range of RSD % was 3.14–10.72%, 5.95–10.81%, 1.32–4.93%, and 1.46–5.51%, respectively (Table S2). The results indicated that the reproducibility of UPLC–QTOF/MS analytical system was acceptable for the metabolic profiling study.

3.4 Discovery and identification of potential metabolites

For supervised multivariate statistical analysis, the Orthogonal Partial Least Squares-Discriminant Analysis (OPLS-DA) was performed to identify the differentially expressed urinary metabolites (Fig. 2). In this work, the four models presented a goodness-of-fit parameter greater than 93.4% (R2Y 0.934–0.979) and a predictability parameter greater than 67.1% (Q2Y 0.671–0.743), which indicated that these OPLS-DA models were established successfully to represent the differentially expressed urinary metabolites between ONFH group and control group. Compared to the controls, 33 differentially expressed urinary metabolites with critical P value < 0.05 and VIP value > 1 in OPLS-DA analysis were significantly changed in ONFH group. The identification of these potential metabolites is based on accurate mass, retention time, MS and MS/MS information by way of comparing the MS and MS/MS spectra structure message. The identified metabolites were depicted in Table 1. The correlations between the relative abundance of validated metabolites and the urine specimens were examined by correlation coefficients (Fig. 3).

3.5 Metabolism pathway analysis

With the aim to illuminate the underlying relevance between the 33 identified metabolites and the osteonecrosis of the femoral head, the most relevant pathways of the tentatively

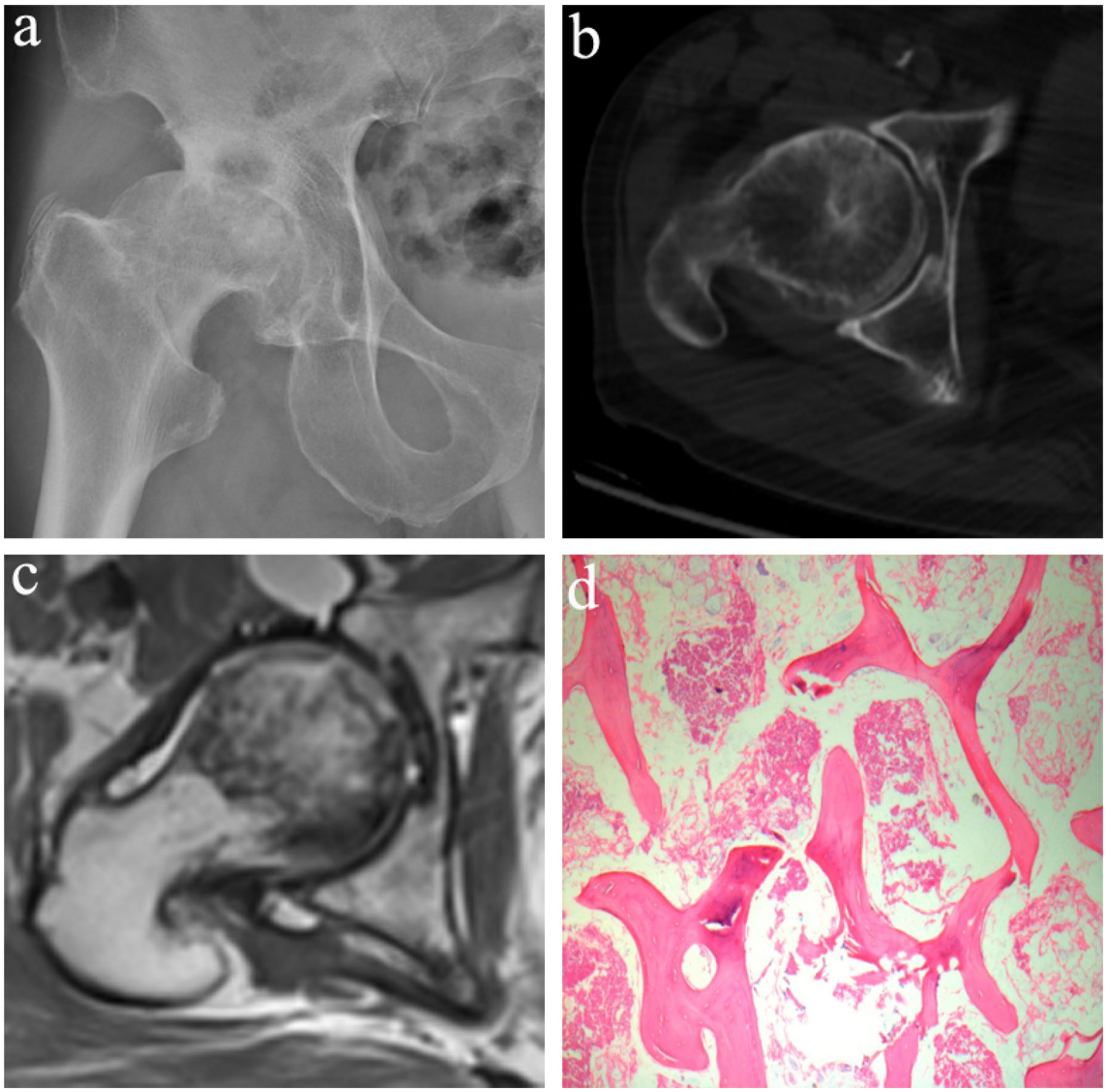

Fig. 1 Radiograph, CT, MRI and histological image (×4) of ONFH samples. **a, b, c** are the X-ray, CT, MRI images of the femoral head from ONFH patients. In **d**, pathological section showed the lesion region of ONFH femoral head

assigned metabolites were identified using the metabolic pathway analysis (MetPA). Metabolic pathway analysis revealed that Sulfur metabolism, Cysteine and methionine metabolism, Glycerophospholipid metabolism, and Histidine metabolism were most relevant to the ONFH (Fig. 4).

3.6 Screening for potential biomarkers

In this work, the differential metabolites with VIP > 1 and AUC (area under the curve of ROC) > 0.85 in ONFH group were picked out as the potential biomarkers. Thus, after the binary logistic regression analysis, Sulfate (AUC 0.882, Fold − 2.0, VIP 2.11), Urea (AUC 0.891, Fold − 1.5, VIP 2.8), Deoxycholic acid (AUC 0.947, Fold − 1.3, VIP 2.66) and PE(14:0/14:1(9Z)) (AUC 0.916, Fold − 1.2, VIP 1.44),were finally pick out as the potential biomarkers using the receiver operating characteristic (ROC) curve to estimate specificity and sensitivity via SPSS19.0 version software. The ROC curves and discriminatory plots of potential biomarkers were displayed in Fig. 5.

4 Discussion

In this study, urinary metabolomics was performed to identify the metabolomic characteristics of ONFH patients. The urinary metabolic profiling of ONFH group was significantly separated from the control group by multivariate statistical analysis. It indicated that the metabolic state of necrotic femoral head had been changed. While the causal relationship

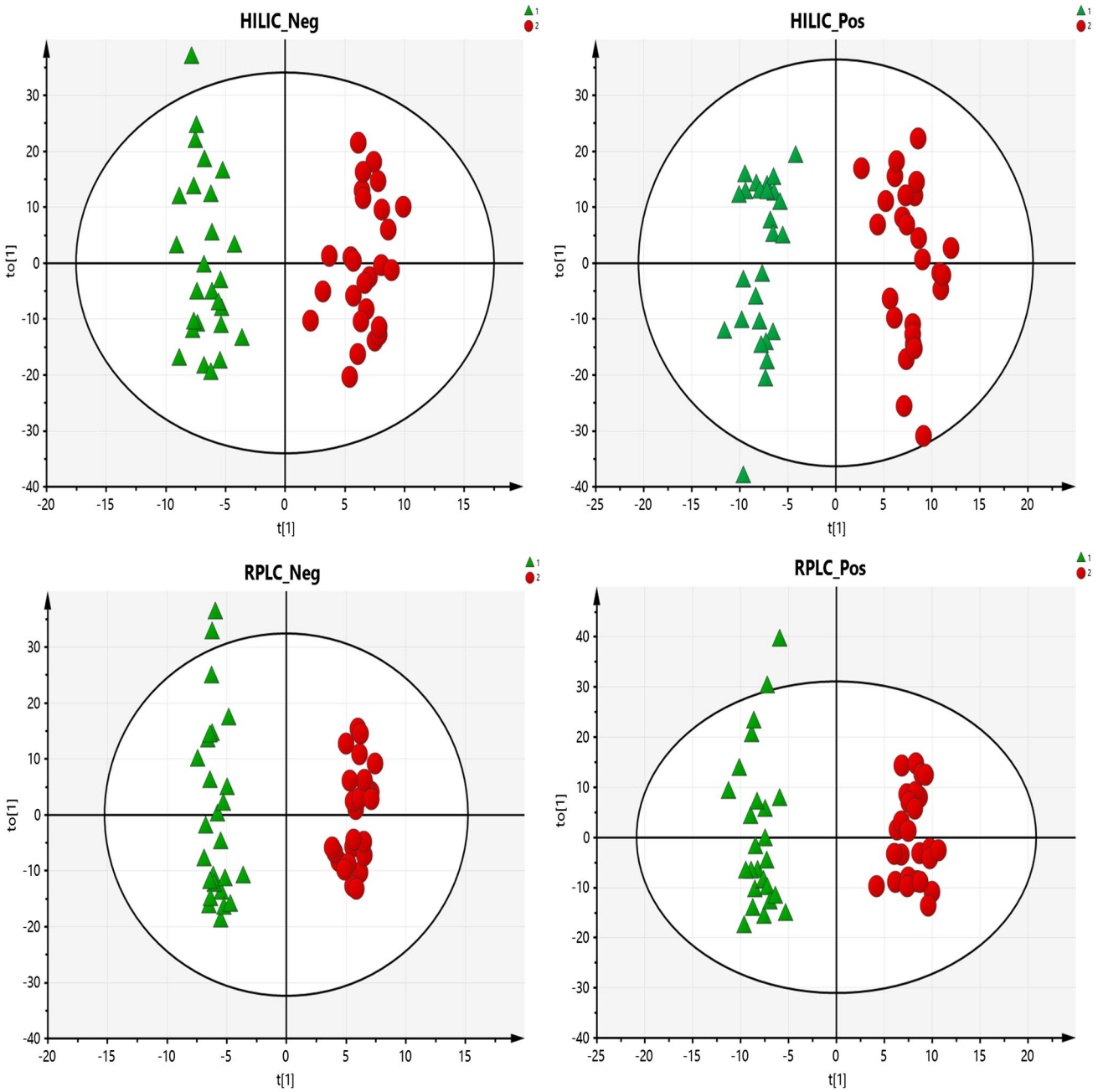

Fig. 2 OPLS-DA score plots of four modes based on urinary metabolic profiling of the ONFH group (triangles) and control group (circles). HILIC_Neg mode, R2Y = 0.948, Q2 = 0.671; HILIC_Pos mode, R2Y = 0.946, Q2 = 0.69; RPLC_Neg mode, R2Y = 0.979, Q2 = 0.737; RPLC_Pos mode, R2Y = 0.934, Q2 = 0.743

between metabolic state changes and ONFH needs further research to confirm. Through the unsupervised principle component analysis of 64 QC samples and relative standard deviation (RSD%) of eight randomly picked peaks in six within-run QC samples, the repeatability and stability of UPLC–QTOF/MS analytical system were acceptable. Therefore, the data in this experiment was reliable. 33 distinctly differential metabolites were identified between the ONFH patients and healthy people, by the way of MS match, MS/MS match, and standard materials match. In which, 9-decenoylcarnitine and 2-*trans*,4-*cis*-decadienoylcarnitine were identified in two different ion modes. Sulfate, urea, deoxycholic acid and PE(14:0/14:1(9Z)) were screened as the potential biomarkers of ONFH. In addition, The results of bioinformatics analysis suggested that sulfur metabolism, cysteine and methionine metabolism, glycerophospholipid

Table 1 List of the identified metabolites between ONFH patients and healthy controls

Metabolites	Mode	Mass (Da)	RT[a] (min)	Error[b] (ppm)	MS/MS[c] (Da)	VIP[d]	P[e]	Formula	Fold change[f]
Sulfate	H-N	96.9615	3.42	4.6	96.9596	2.10926	0.002	H_2O_4S	0.495
Citric acid	H-N	191.0211	6.3	0.4	111.0082	1.53812	0.028	$C_6H_8O_7$	1.641
3,7-Dimethyluric acid	H-N	195.0522	5.56	− 0.3	41.9985	1.43688	0.040	$C_7H_8N_4O_3$	1.483
2-Methylbutyrylglycine	H-N	158.0830	2.47	6.3	57.5290	1.39541	0.000	$C_7H_{13}NO_3$	0.469
(*S*)-3,4-dihydroxybutyric acid	H-N	119.0360	1.14	0.2	59.0133	1.37529	0.023	$C_4H_8O_4$	1.441
L-Serine	H-N	104.0366	4.51	0.5	73.8010	1.1778	0.015	$C_3H_7NO_3$	1.410
L-Histidine	H-N	154.0636	4.9	0.6	153.9962	1.14513	0.000	$C_6H_9N_3O_2$	1.411
Peroxynitrite	H-N	61.99150	3.36	0.5	61.9876	1.50834	0.031	HNO_3	1.305
Urea	H-P	61.04150	3.67	0.5	61.0427	2.81661	0.000	CH_4N_2O	0.676
Asymmetric dimethylarginine	H-P	203.1523	5.05	− 1	88.0875	2.08443	0.000	$C_8H_{18}N_4O_2$	0.584
*N*2-methylguanine	H-P	166.0739	4.06	− 0.7	95.0245	1.90448	0.001	$C_6H_7N_5O$	0.587
Homocysteine	H-P	136.0495	3.82	− 0.8	47.2160	1.82478	0.002	$C_4H_9NO_2S$	1.754
Succinyladenosine	H-P	384.1164	3.56	0.1	204.0521	1.67597	0.005	$C_{14}H_{17}N_5O_8$	0.536
3-Hydroxy-*N*6,*N*6,*N*6-trimethyl-L-lysine	H-P	205.1563	5.37	0.8	74.0964	1.60694	0.007	$C_9H_{21}N_2O_3$	0.642
Phenylacetylglutamine	H-P	265.1197	3.41	− 2.2	28.0187	1.57953	0.008	$C_{13}H_{16}N_2O_4$	0.414
*N*6-methyladenosine	H-P	282.1212	4.49	0.2	150.0768	1.55618	0.009	$C_{11}H_{15}N_5O_4$	0.721
L-Histidine	H-P	156.0784	4.87	− 0.4	156.0772	1.53571	0.010	$C_6H_9N_3O_2$	0.638
o-Tyrosine	H-P	182.0805	4.71	− 0.8	79.0542	1.45581	0.016	$C_9H_{11}NO_3$	2.168
*N*6,*N*6,*N*6-trimethyl-L-lysine	H-P	189.1613	5.45	0.9	74.0964	1.38362	0.022	$C_9H_{20}N_2O_2$	0.743
9-Decenoylcarnitine[g]	H-P	314.2334	3.78	0.5	144.1019	1.37003	0.025	$C_{17}H_{31}NO_4$	1.797
2-*trans*,4-*cis*-Decadienoylcarnitine[g]	H-P	312.2179	3.75	0.2	155.3255	1.35565	0.025	$C_{17}H_{29}NO_4$	1.669
1-Methylnicotinamide	H-P	137.0724	4.59	− 0.5	94.0662	1.32992	0.028	$C_7H_9N_2O$	0.621
1-Methylhistidine	H-P	170.0938	5.98	0.2	109.300	1.29845	0.035	$C_7H_{11}N_3O_2$	2.372
Creatinine	H-P	114.0673	2.52	0.5	114.0667	1.26759	0.040	$C_4H_7N_3O$	0.341
Sebacic acid	R-N	201.1135	3.47	0.8	129.999	1.32794	0.004	$C_{10}H_{18}O_4$	2.005
Dextrorphan *O*-glucuronide	R-N	432.1952	3.36	1	256.1707	1.27361	0.000	$C_{23}H_{31}NO_7$	2.369
Capryloylglycine	R-N	200.1295	3.61	0.8	67.6820	1.21748	0.000	$C_{10}H_{19}NO_3$	1.582
Androsterone glucuronide	R-N	465.2496	4.06	0.7	289.2168	1.20782	0.000	$C_{25}H_{38}O_8$	1.538
Hippuric acid	R-N	178.0520	2.31	− 1	77.0381	1.10295	0.000	$C_9H_9NO_3$	0.534
Deoxycholic acid	R-P	393.2969	7.9	− 0.2	273.7795	2.6632	0.000	$C_{24}H_{40}O_4$	0.755
Dihydrovaltrate	R-P	425.2145	6.35	0.9	57.0704	1.78405	0.000	$C_{22}H_{32}O_8$	0.849
PE(14:0/14:1(9Z))	R-P	634.4517	5.97	1	493.4257	1.43856	0.003	$C_{33}H_{64}NO_8P$	0.822
2-*trans*,4-*cis*-Decadienoylcarnitine[g]	R-P	312.2170	3.15	− 0.6	142.1317	1.33233	0.006	$C_{17}H_{29}NO_4$	2.051
9-Decenoylcarnitine[g]	R-P	314.2328	3.33	0.5	144.1019	1.18075	0.017	$C_{17}H_{31}NO_4$	2.030
Glycerol 3-phosphate	R-P	173.0127	8.97	− 0.9	149.0261	1.82157	0.000	$C_3H_9O_6P$	0.847

[a]Retention time of features

[b]Mass error calculated by using experimental mass minus theoretical mass

[c]Matched MS/MS peaks with highest intensity

[d]The variable importance in projection value of OPLS-DA models

[e]Performed using signed-rank test by the SPSS19.0 software

[f]Compared ONFH group with control group

[g]Found in two or more analytic modes

metabolism, and histidine metabolism might be associated with the pathogenic progress of ONFH. These findings indicated that the urinary metabolomics could be an important way for the biomarker discovery and pathological mechanism research of ONFH.

Based on the binary logistic regression analysis, sulfate, urea, deoxycholic acid and PE(14:0/14:1(9Z)) were screened as the potential biomarkers of ONFH. The sulfate ion is a polyatomic anion with the empirical formula SO_4^{2-}, which could combine with calcium to form the calcium sulfate

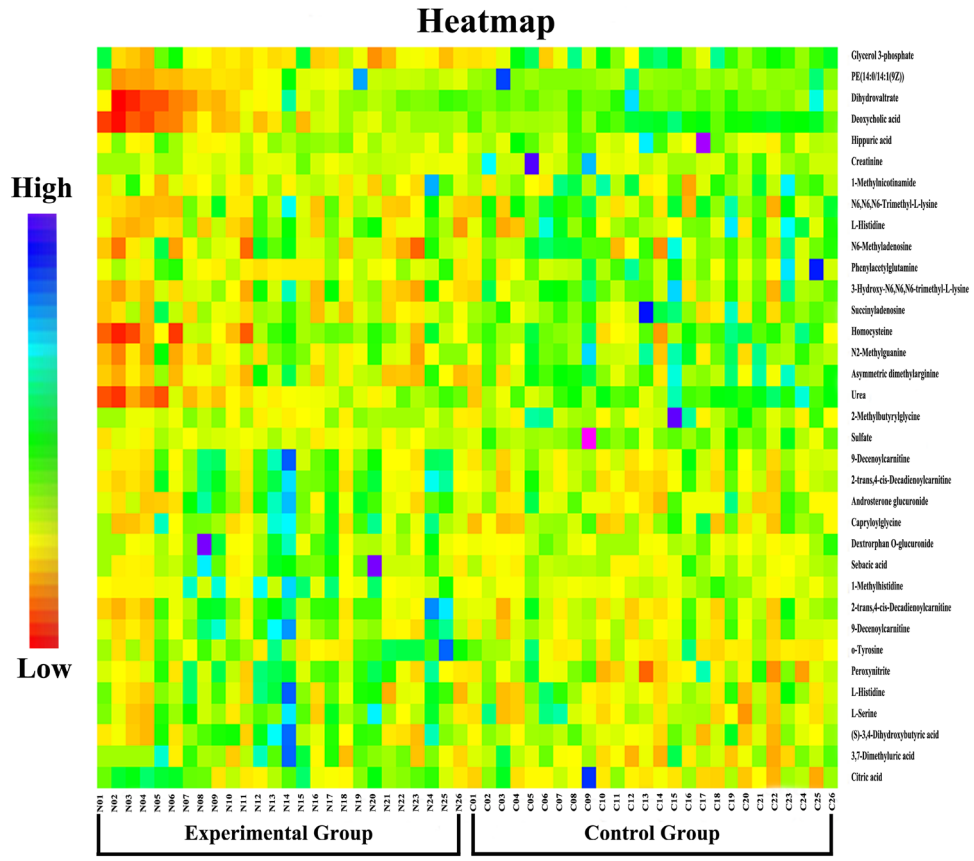

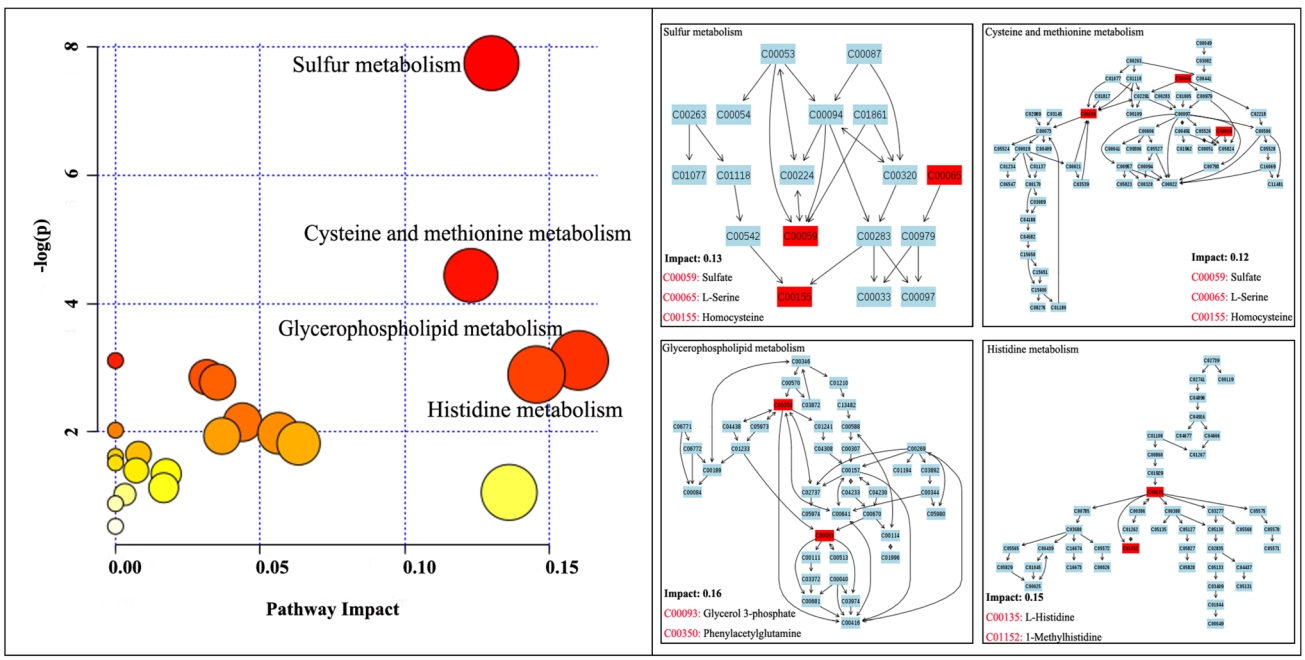

Fig. 3 The correlation heatmap between the level of identified metabolites and the samples

Fig. 4 Metabolic pathway analysis of the identified metabolites in urine of ONFH patients. Sulfur metabolism (PI = 0.130), Cysteine and methionine metabolism (PI = 0.123), Glycerophospholipid metabolism (PI = 0.160) and Histidine metabolism (P = 0.146) were recognized by using MetaboAnalyst 4.0

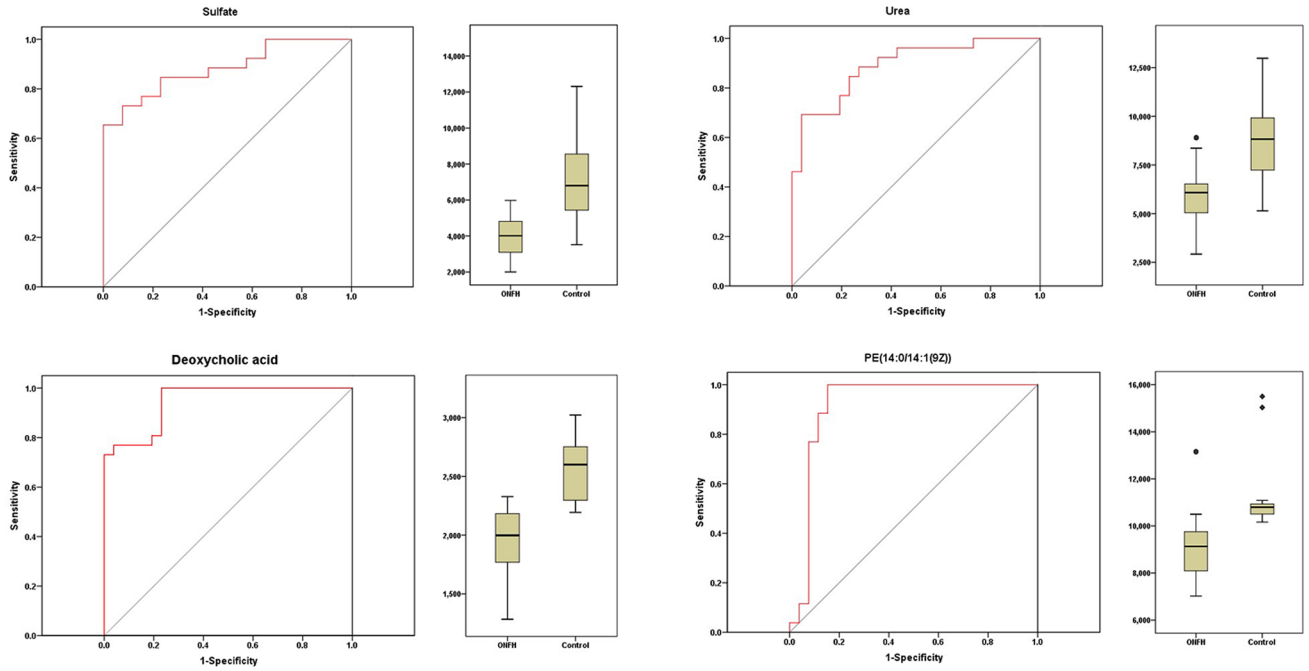

Fig. 5 The receiver operating characteristic (ROC) curves and discriminatory plots of potential biomarkers. Sulfate (AUC 0.882, Fold − 2.0, VIP 2.11), Urea (AUC 0.891, Fold − 1.5, VIP 2.8), Deoxycholic acid (AUC 0.947, Fold − 1.3, VIP 2.66) and PE(14:0/14:1(9Z)) (AUC 0.916, Fold − 1.2, VIP 1.44)

($CaSO_4$). In recent years, calcium sulfate ($CaSO_4$)/calcium phosphate ($CaPO_4$) are successfully employed as synthetic bone graft for the treatment of contained defects in early-stage ONFH patients by enhancing its bone forming properties (Sionek et al. 2018; Civinini et al. 2017). Urea is the principal end product of protein catabolism, which is produced by the deamination of amino acids known simply as the urea cycle (Lee et al. 2018). It has no physiological function. It may represent the body's high catabolic state of protein. Deoxycholic acid is a secondary bile acid, which facilitates fat absorption and cholesterol excretion (Wang et al. 2006). Deoxycholic acid was a potent apoptotic inducer and had been confirmed as tumor promoter(Qiao et al. 2001; Lim et al. 2012), which might be related to the apoptosis of bone cells in ONFH patients. PE(14:0/14:1(9Z)) is a glycerophospholipid in which a phosphorylethanolamine moiety occupies a glycerol substitution site. The study presented by Kilpinen et al. (2013) suggested that aging bone marrow mesenchymal stromal cells had altered membrane glycerophospholipids composition and functionality. These discoveries indicated that the disordered glycerophospholipids might play a vital role in the intercellular signal transduction and bones cell apoptotic process.

The results of bioinformatics analysis indicated that glycerophospholipid metabolism was significantly disturbed in ONFH. Metabolic pathway analysis revealed that glycerol 3-phosphate and phenylacetylglutamine belonged to the glycerophospholipid metabolism. Glycerophospholipids were synthesized from glycerol 3-phosphate (G3P) in a de novo pathway (Hishikawa et al. 2014). Glycerophospholipids were ubiquitous cell membrane components and play important roles in the development and function of several tissues (Chierico et al. 2014). It could modulate transmembrane signaling and mediate cell-to-cell and cell-tomatrix interactions (Seito et al. 2012). Glycerophospholipids metabolism participated in the regulation of many cellular processes such as cell proliferation, growth, differentiation, survival, apoptosis, motility, inflammation, membrane homeostasis (Huang et al. 2015). In aging bone marrow mesenchymal stromal cells, the membrane glycerophospholipid composition and functionality were altered (Kilpinen et al. 2013). In addition, glycerophospholipids occupied a large part of the distinctive metabolites in serum and bone tissue of osteonecrosis femoral head from ONFH patients using UPLC–MS/MS (Xu et al. 2017; Zhu et al. 2016). Thus, these results suggested that glycerophospholipid metabolism played a vital regulation role in the pathological process of osteonecrosis femoral head.

The results of bioinformatics analysis indicated that histidine metabolism was significantly changed in ONFH. Metabolic pathway analysis revealed that L-histidine and 1-methylhistidine were hit in the histidine metabolism with an impact factor of 0.15. Histidine was an essential amino acids in mammals. It played enormous biological importance in hemoglobin structure and function, protein methylation, antioxidative dipeptides, and one-carbon unit metabolism

(Wu et al. 2009; Blachier et al. 2007). Thereby, histidine could regulate the gene expression and the biological activity of proteins. In addition, histidine was an important component of mammalian histidine kinases and histidine phosphorylated proteins (Klumpp et al. 2002), which are likely to contribute to our understanding of the signal transduction and cancer formation (Steeg et al. 2003). In the osteoclast, the protein T cell ubiquitin ligand-2 (TULA-2), a novel histidine phosphatases, was abundantly expressed. TULA-2 negatively regulated osteoclast differentiation and function (Back et al. 2013). 1-Methylhistidine had be used for monitoring the muscle protein catabolism by UPLC-MS/MS in human urine (Wang et al. 2012). The results presented by Aranibar et al. (2011) indicated that 1-methylhistidine might be an useful urine and serum biomarker of hypertrophy and drug-induced skeletal muscle toxicity in rat. Overall, the role of histidine metabolism in osteonecrosis of the femoral head remains to be further studied.

The metabolic pathway analysis revealed that cysteine and methionine metabolism was related to ONFH, with L-serine, sulfate and homocysteine hitting in this pathway. The study presented by Ogawa et al. highlighted a novel role for L-serine in RANKL signaling in osteoclastogenesis (Back et al. 2006). And L-serine metabolism was indispensable for osteoclasts to form in vitro (Bahtiar et al. 2009). By contrast, L-serine promoted osteoclastic differentiation in a manner sensitive to the inhibition by D-serine. However, osteoclastogenesis was negatively regulated by D-serine produced by osteoblast (Takarada et al. 2012). In general, L-serine played a promotion role in the osteoclast formation, and thereby inducing bone resorption. Evidence from previous studies showed that homocysteine was known to modulate bone remodeling via several known mechanisms such as increase in osteoclast activity, decrease in osteoblast activity (Koh et al. 2006; Vijayan et al. 2013). In addition, homocysteine performed a detrimental effect on bone via decreasing in bone blood flow and increasing in matrix metalloproteinases that degraded extracellular bone matrix (Blouin et al. 2009; Tyagi et al. 2011). Homocysteine bound directly to extracellular matrix and reduced bone strength (Herrmann et al. 2005). It was suggested that homocysteine was known to cause apoptosis via generation of ROS by the mitochondrial mechanism in osteoblast cells and human bone marrow stromal cells lines (Kim et al. 2006). These discoveries agree with our results of disordered cysteine and methionine metabolism, and suggested that L-serine and homocysteine play a vital regulation role in the pathology process in ONFH.

The subjects included in our study were advanced ONFH patients with a stage III or IV on the Ficat classification. It could not represent the metabolic profiling of early ONFH patients. Therefore, its usefulness in early diagnosis for ONFH need further identification. Low number of ONFH patients was another limitation of this study. In addition, four potential biomarkers were detected in different conditions. It would theoretically imply some practical limitations in the detection of all the potential biomarkers in same method. Our future work will dedicate to discover the potential relationships between the differential metabolites and the early onset of disease in early ONFH patient with a stage I or II on the Ficat classification. In addition, these differential metabolites will be further identified in large amount of urine and serum samples, with the aim to confirm the diagnostic biomarkers of ONFH.

5 Conclusions

At present, the approach based on UPLC-QTOF/MS metabolomics, highlight the power for studying the urinary metabolic profiling of ONFH patients and healthy people. The identified 33 potential metabolites and four potential biomarkers, were found to be distinctly different between the ONFH patients and healthy people. It is noteworthy that the metabolites compositions discovered between ONFH patients and controls could suggest the variation of the disease. Sulfate, urea, deoxycholic acid and PE(14:0/14:1(9Z)) were screened as the potential biomarkers of ONFH. Our results suggested that sulfur metabolism, cysteine and methionine metabolism, glycerophospholipid metabolism, and histidine metabolism might be associated with the pathogenic progress of ONFH. The results of bioinformatics analysis indicated a disturbance in the signal transduction, membrane glycerophospholipid composition, bone remodeling, hemodynamics, osteocyte formation and apoptosis in ONFH patients. This metabolomic study provided a new feasible way to explore the pathological mechanism of ONFH. And more work will be needed to clarify the complex pathological mechanism. Further validation of these differential metabolites and metabolism mechanisms would be considerable in larger amount of subjects.

Compliance with ethical standards

Conflict of interest The authors declare no conflict of interest.

Human and animal rights All procedures performed in studies involving human participants were in accordance with the ethical standards of the institutional and/or national research committee and with the 1964 Helsinki declaration and its later amendments or comparable ethical standards.

Informed consent Informed consent was obtained from all participants included in the study.

References

Aranibar, N., Vassallo, J. D., Rathmacher, J., et al. (2011). Identification of 1- and 3-methylhistidine as biomarkers of skeletal muscle toxicity by nuclear magnetic resonance-based metabolic profiling. *Analytical Biochemistry, 410*(1), 84–91.

Back, S. H., Adapala, N. S., Barbe, M. F., Carpino, N. C., Tsygankov, A. Y., & Sanjay, A. (2006). A novel role of L-serine (L-Ser) for the expression of nuclear factor of activated T cells (NFAT)2 in receptor activator of nuclear factor kB ligand (RANKL)-induced osteoclastogenesis in vitro. *Journal of Bone and Mineral Metabolism, 24*(5), 373–379.

Back, S. H., Adapala, N. S., Barbe, M. F., Carpino, N. C., Tsygankov, A. Y., & Sanjay, A. (2013). TULA-2, a novel histidine phosphatase regulates bone remodeling by modulating osteoclast function. *Cellular and Molecular Life Sciences, 70*(7), 1269–1284.

Bahtiar, A., Matsumoto, T., Nakamura, T., et al. (2009). Identification of a novel L-serine analog that suppresses osteoclastogenesis in vitro and bone turnover in vivo. *Journal of Biological Chemistry, 284*(49), 34157–34166.

Bijlsma, S., Bobeldijk, I., Verheij, E. R., et al. (2006). Large-scale human metabolomics studies: A strategy for data (pre-) processing and validation. *Analytical Chemistry, 78*, 567–574.

Blachier, F., Mariotti, F., Huneau, J. F., & Tome´, D. (2007). Effects of amino acid-derived luminal metabolites on the colonic epithelium and physiopathological consequences. *Amino Acids, 33*, 547–562.

Blouin, S., Thaler, H. W., Korninger, C., et al. (2009). Bone matrix quality and plasma homocysteine levels. *Bone, 44*, 959–964.

Calder, J. D., Buttery, L., Revell, P. A., Pearse, M., & Polak, J. M. (2004). Apoptosis—A significant cause of bone cell death in osteonecrosis of the femoral head. *Journal of Bone and Joint Surgery British, 86*(8), 1209–1213.

Chierico, L., Joseph, A. S., Lewis, A. L., & Battaglia, G. (2014). Live cell imaging of membrane/cytoskeleton interactions and membrane topology. *Science Report, 4*, 6056.

Civinini, R., Capone, A., Carulli, C., Matassi, F., Nistri, L., & Innocenti, M. (2017). The kinetics of remodeling of calcium sulfate/calcium phosphate bioceramic. *Journal of Materials Science: Materials in Medicine, 28*(9), 137.

Cui, L., Zhuang, Q., Lin, J., et al. (2016). Multicentric epidemiologic study on six thousand three hundred and ninety five cases of femoral head osteonecrosis in China. *International Orthopaedics, 40*(2), 267–276.

De Preter, V. (2015). Metabonomics and systems biology. *Methods in Molecular Biology, 1277*, 245–255.

Glueck, C. J., Freiberg, R. A., & Wang, P. (2008). Heritable thrombophilia-hypofibrinolysis and osteonecrosis of the femoral head. *Clinical Orthopaedics and Related Research, 466*, 1034–1040.

Grauso, L., Mariggio, S., Corda, D., Fontana, A., & Cutignano, A. (2015). An improved UPLC–MS/MS platform for quantitative analysis of glycerophosphoinositol in mammalian cells. *PLoS One, 10*, e0123198.

Hernigou, P., Flouzat-Lachaniette, C. H., & Delambre, J. (2015). Osteonecrosis repair with bone marrow cell therapies: State of the clinical art. *Bone, 70*, 102–109.

Herrmann, M., Widmann, T., & Herrmann, W. (2005). Homocysteine—A newly recognised risk factor for osteoporosis. *Clinical Chemistry and Laboratory Medicine, 43*, 1111–1117.

Hishikawa, D., Hashidate, T., Shimizu, T., & Shindou, H. (2014). Diversity and function of membrane glycerophospholipids generated by the remodeling pathway in mammalian cells. *Journal of Lipid Research, 55*(5), 799–807.

Holmes, E., Wilson, I. D., & Nicholson, J. K. (2008). Metabolic phenotyping in health and disease. *Cell, 134*, 714–717.

Huang, C., & Freter, C. (2015). Lipid metabolism, apoptosis and cancer therapy. *International Journal of Molecular Sciences, 16*(1), 924–949.

Issaq, H. J., Van, Q. N., Waybright, T. J., Muschik, G. M., & Veenstra, T. D. (2009). Analytical and statistical approaches to metabolomics research. *Journal of Separation Science, 32*, 2183–2199.

Kang, P., Xie, X., Tan, Z., Yang, J., Shen, B., Zhou, Z., & Pei, F. (2015). Repairing defect and preventing collapse of femoral head in a steroid-induced osteonecrotic of femoral head animal model using strontiumdoped calcium polyphosphate combined BMMNCs. *Journal of Materials Science: Materials in Medicine, 26*(2), 80.

Kilpinen, L., Tigistu-Sahle, F., Oja, S., et al. (2013). Aging bone marrow mesenchymal stromal cells have altered membrane glycerophospholipid composition and functionality. *Journal of Lipid Research, 54*(3), 622–635.

Kim, D. J., Koh, J. M., Lee, O., et al. (2006). Homocysteine enhances apoptosis in human bone marrow stromal cells. *Bone, 39*, 582–590.

Klumpp, S., & Krieglstein, J. (2002). Phosphorylation and dephosphorylation of histidine residues in proteins. *European Journal of Biochemistry, 269*, 1067–1071.

Koh, J. M., Lee, Y. S., Kim, Y. S., et al. (2006). Homocysteine enhances bone resorption by stimulation of osteoclast formation and activity through increased intracellular ROS generation. *Journal of Bone and Mineral Research, 21*(7), 1003–1011.

Lee, J. S., Adler, L., Karathia, H., Carmel, N., Rabinovich, S., Auslander, N., & Keshet, R. (2018). Urea cycle dysregulation generates clinically relevant genomic and biochemical signatures. *Cell, 174*(6), 1559–1570.

Lee, J. S., Roh, H. L., Kim, C. H., Jung, J. S., & Suh, K. T. (2006). Alterations in the differentiation ability of mesenchymal stem cells in patients with nontraumatic osteonecrosis of the femoral head: Comparative analysis according to the risk factor. *Journal of Orthopaedic Research, 24*, 604–609.

Levasseur, R. (2008). Mechanisms of osteonecrosis. *Joint Bone Spine, 75*, 639–642.

Lim, S. C., Duong, H. Q., Parajuli, K. R., & Han, S.I. (2012). Pro-apoptotic role of the MEK/ERK pathway in ursodeoxycholic acid-induced apoptosis in SNU601 gastric cancer cells. *Oncology Report, 28*(4), 1429–1434.

Liu, F., Wang, W., Yang, L., et al. (2017). An epidemiological study of etiology and clinical characteristics in patients with nontraumatic osteonecrosis of the femoral head. *Journal of Research in Medical Sciences, 22*, 15.

Liu, X., Li, Q., Sheng, J., Hu, B., et al. (2016). Unique plasma metabolomic signature of osteonecrosis of the femoral head. *Journal of Orthopaedic Research, 34*, 1158–1167.

Loscalzo, J., Kohane, I., & Barabasi, A. L. (2007). Human disease classification in the postgenomic era: A complex systems approach to human pathobiology. *Molecular Systems Biology, 3*, 124.

Mankin, H. J. (1992). Nontraumatic necrosis of bone (osteonecrosis). *The New England Journal of Medicine, 326*, 1473–1479.

Moya-Angeler, J., Gianakos, A. L., Villa, J. C., Ni, A., & Lane, J. M. (2015). Current concepts on osteonecrosis of the femoral head. *World Journal of Orthopedics, 6*(8), 590–601.

Patti, G. J., Yanes, O., & Siuzdak, G. (2012). Innovation: metabolomics: The pogee of the omics trilogy. *Nature Reviews Molecular Cell Biology, 13*, 263–269.

Powell, C., Chang, C., & Gershwin, M. E. (2011). Current concepts on the pathogenesis and natural history of steroid-induced osteonecrosis. *Clinical Reviews in Allergy & Immunology, 41*(1), 102–113.

Puchades-Carrasco, L., & Pineda-Lucena, A. (2015). Metabolomics in pharmaceutical research and development. *Current Opinion in Biotechnology, 35*, 73–77.

Qiang, H., Liu, H., Ling, M., Wang, K., & Zhang, C. (2015). Early steroid-induced osteonecrosis of rabbit femoral head and *Panax notoginseng* saponins: Mechanism and protective effects. *Evidence-Based Complementary and Alternative Medicine*, 2015, 719370.

Qiao, L., Studer, E., Leach, K., et al. (2001). Deoxycholic acid (DCA) causes ligand-independent activation of epidermal growth factor receptor (EGFR) and FAS receptor in primary hepatocytes: Inhibition of EGFR/mitogen-activated protein kinase-signaling module enhances DCA-induced apoptosis. *Mol Biol Cell, 12*, 2629–2645.

Ragab, Y., Emad, Y., & Abou-Zeid, A. (2008). Bone marrow edema syndromes of the hip: mRI features in different hip disorders. *Clinical Rheumatology, 27*(4), 475–482.

Schuhmacher, R., Krska, R., Weckwerth, W., & Goodacre, R. (2013). Metabolomics and metabolite profiling. *Analytical and Bioanalytical Chemistry, 405*, 5003–5004.

Seito, N., Yamashita, T., Tsukuda, Y., et al. (2012). Interruption of glycerophospholipids synthesis enhances osteoarthritis development in mice. *Arthritis & Rheumatology, 64*(8), 2579–2588.

Shah, K. N., Racine, J., Jones, L. C., & Aaron, P. K. (2015). Pathophysiology and risk factors for osteonecrosis. *Current Reviews in Musculoskeletal Medicine, 8*, 201–209.

Sionek, A., Czwojdziński, A., Kowalczewski, J., et al. (2018). Hip osteonecroses treated with calcium sulfate-calcium phosphate bone graft substitute have different results according to the cause of osteonecrosis: Alcohol abuse or corticosteroid-induced. *International Orthopaedics, 42*(7), 1491–1498.

Slobogean, G. P., Sprague, S. A., Scott, T., & Bhandari, M. (2015). Complications following young femoral neck fractures. *Injury, 46*(3), 484–491.

Snyder, M., & Li, X. Y. (2013). Metabolomics as a robust tool in systems biology and personalized medicine: An open letter to the metabolomics community. *Metabolomics, 3*, 532–534.

Steeg, P. S., Palmieri, D., Ouatas, T., & Salerno, M. (2003). Histidine kinases and histidine phosphorylated proteins in mammalian cell biology, signal transduction and cancer. *Cancer Letter, 190*(1), 11–12.

Stevens, K., Tao, C., Lee, S. U., et al. (2003). Subchondral fractures in osteonecrosis of the femoral head: Comparison of radiography, CT, and MR imaging. *AJR American Journal of Roentgenology, 180*, 363–368.

Sugano, N., Kubo, T., & Takaoka, K. (1999). Diagnostic criteria for non-traumatic osteonecrosis of the femoral head: A multicentre study. *Journal of Bone and Joint Surgery British, 81*, 590–595.

Takarada, T., Takarada-Iemata, M., Takahata, Y., et al. (2012). Osteoclastogenesis is negatively regulated by D-serine produced by osteoblasts. *Journal of Cellular Physiology, 227*(10), 3477–3487.

Tyagi, N., Kandel, M., Munjal, C., et al. (2011). Homocysteine mediated decrease in bone blood flow and remodeling: Role of folic acid. *Journal of Orthopaedic Research, 29*, 1511–1516.

Vijayan, V., Khandelwal, M., Manglani, K., Singh, R. R., Gupta, S., & Surolia, A. (2013). Homocysteine alters the osteoprotegerin/RANKL system in the osteoblast to promote bone loss: Pivotal role of the redox regulator forkhead O1. *Free Radical Biology & Medicine, 61*, 72–84.

Wang, H., Hu, P., & Jiang, J. (2012). Measurement of 1- and 3-methylhistidine in human urine by ultra performance liquid chromatography–tandem mass spectrometry. *Clinica Chimica Acta, 413*(1–2), 131–138.

Wang, Y., Jones, P. J., Woollett, L. A., et al. (2006). Effects of chenodeoxycholic acid and deoxycholic acid on cholesterol absorption and metabolism in humans. *Translational Research, 148*(1), 37–45.

Want, E. J., Wilson, I. D., Gika, H., et al. (2010). Global metabolic profiling procedures for urine using UPLC–MS. *Nature Protocols, 5*(6), 1005–1018.

Wen, Z., Lin, Z., Yan, W., & Zhang, J. (2017). Influence of cigarette smoking on osteonecrosis of the femoral head (ONFH): A systematic review and meta-analysis. *Hip International, 27*(5), 425–435.

Wilson, I. (2014). Tools for systems biology. *Bioanalysis, 6*(19), 2517–2518.

Winder, C. L., Cornmell, R., Schuler, S., Jarvis, R. M., Stephens, G. M., & Goodacre, R. (2011). Metabolic fingerprinting as a tool to monitor whole-cell biotransformations. *Analytical and Bioanalytical Chemistry, 399*, 387–401.

Wu, G. (2009). Amino acids: Metabolism, functions, and nutrition. *Amino Acids, 37*(1), 11–17.

Xu, Z. W., Xu, K. M., Ding, S. J., et al. (2017). Serum metabolomic study for detecting biomarkers of non-traumatic osteonecrosis of the femoral head. *Metabolomics, 13*, 73.

Zalavras, C., Dailiana, Z., Elisaf, M., et al. (2000). Potential aetiological factors concerning the development of osteonecrosis of the femoral head. *European Journal of Clinical Investigation, 30*, 215–221.

Zalavras, C. G., & Lieberman, J. R. (2014). Osteonecrosis of the femoral head: Evaluation and treatment. *Journal of the American Academy of Orthopaedic Surgeons, 22*(7), 455–464.

Zhang, A., Sun, H., Wang, P., Han, Y., & Wang, X. (2012). Future perspectives of personalized medicine in traditional Chinese medicine: a systems biology approach. *Complementary Therapies in Medicine, 20*, 93–99.

Zhu, W. W., Chen, T. M., Ding, S. J., et al. (2016). Metabolomic study of the bone trabecula of osteonecrosis femoral head patients based on UPLC–MS/MS. *Metabolomics, 12*, 48.